ISSN 1674-1056
http://cpb.iphy.ac.cn
http://iopscience.iop.org/cpb
中国物理 B
Chinese Physics
中国物理
Chinese Physics B

Unusual softening behavior of yield strength in niobium at high pressures

Qiu-Min Jing(敬秋民), Qiang He(何强), Yi Zhang(张毅), Shou-Rui Li(李守瑞), Lei Liu(柳雷), Qi-Yue Hou(侯琪玥), Hua-Yun Geng(耿华运), Yan Bi(毕延), Yu-Ying Yu(俞宇颖), Qiang Wu(吴强)

Citation: Chin. Phys. B . 2018, 27(10): 106201. **doi:** 10.1088/1674-1056/27/10/106201

Journal homepage: http://cpb.iphy.ac.cn; http://iopscience.iop.org/cpb

What follows is a list of articles you may be interested in

Neutron powder diffraction and high-pressure synchrotron x-ray diffraction study of tantalum nitrides

Lei-hao Feng(冯雷豪), Qi-wei Hu(胡启威), Li Lei(雷力), Lei-ming Fang(房雷鸣), Lei Qi(戚磊), Lei-lei Zhang(张雷雷), Mei-fang Pu(蒲梅芳), Zi-li Kou(寇自力), Fang Peng(彭放), Xi-ping Chen(陈喜平), Yuan-hua Xia(夏元华), Yohei Kojima(小岛洋平), Hiroaki Ohfuji(大藤宏明), Duan-wei He(贺端威), Bo Chen(陈波), Tetsuo Irifune(入舩徹男)

Chin. Phys. B . 2018, 27(2): 026201. **doi:** 10.1088/1674-1056/27/2/026201

Exploring the compression behavior of HP-$BiNbO_4$ under high pressure

Yin-Juan Liu(刘银娟), Jia-Wei Zhang(张佳威), Duan-Wei He(贺端威), Chao Xu(许超), Qi-Wei Hu(胡启威), Lei Qi(戚磊), A-Kun Liang(梁阿坤)

Chin. Phys. B . 2017, 26(11): 116202. **doi:** 10.1088/1674-1056/26/11/116202

How to detect melting in laser heating diamond anvil cell

Liuxiang Yang(杨留响)

Chin. Phys. B . 2016, 25(7): 076201. **doi:** 10.1088/1674-1056/25/7/076201

Ruby fluorescence pressure scale: Revisited

Liu Lei, Bi Yan, Xu Ji-An

Chin. Phys. B . 2013, 22(5): 056201. **doi:** 10.1088/1674-1056/22/5/056201

First-order character of the displacive structural transition in $BaWO_4$

Tan Da-Yong, Xiao Wan-Sheng, Zhou Wei, Chen Ming, Xiong Xiao-Lin, Song Mao-Shuang

Chin. Phys. B . 2012, 21(8): 086201. **doi:** 10.1088/1674-1056/21/8/086201

Unusual softening behavior of yield strength in niobium at high pressures*

Qiu-Min Jing(敬秋民)†, Qiang He(何强), Yi Zhang(张毅), Shou-Rui Li(李守瑞), Lei Liu(柳雷), Qi-Yue Hou(侯琪玥), Hua-Yun Geng(耿华运), Yan Bi(毕延), Yu-Ying Yu(俞宇颖), and Qiang Wu(吴强)

National Key Laboratory of Shock Wave and Detonation Physics, Institute of Fluid Physics, China Academy of Engineering Physics, Mianyang 621900, *China*

(Received 19 May 2018; revised manuscript received 9 July 2018; published online 10 September 2018)

In situ synchrotron angle-dispersive x-ray diffraction experiments on niobium powders have been conducted at pressures up to 61 GPa and room temperature using the diamond anvil cell technique. From the full width at half maximum of the measured diffraction lines, the yield strength was derived with the line-width analysis theory. The niobium powder sample was found to be compressed more packed firstly and then yielded at ~ 14 GPa–18 GPa. Following an initial increase in the yield strength with pressure, an obvious decrease was observed occurring at ~ 42 GPa–47 GPa accompanying with a typical pressure dependence above 47 GPa. The experimentally observed anomalous softening of the yield strength in niobium surprisingly follows the trend of the predicted unusual softening in the shear modulus by the recent theoretical investigations. The possible mechanisms, applicable to interpret the yield strength softening of materials at high pressure, were also discussed in detail.

Keywords: x-ray diffraction, niobium, diamond anvil cell, yield strength, anomalous softening

PACS: 62.50.–p, 07.35.+k, 62.20.F–, 64.30.Ef **DOI:** 10.1088/1674-1056/27/10/106201

1. Introduction

Recently, the group-VB transition metals (V, Nb, and Ta) have attracted numerous theoretical and experimental studies[1–10] due to their unusual mechanical properties associated with the peculiar electronic band structure effects under pressure. Theoretical studies[1–3] predicted a pronounced softening in the trigonal shear modulus C_{44} of the body-centered cubic (bcc) VB metals, driving a mechanical instability in vanadium while only pressure softening of the shear modulus in niobium and tantalum. The predicted structural transition in vanadium was later confirmed by experiments,[4–6] as well as by other theoretical studies.[7–9] *In situ* synchrotron x-ray diffraction (XRD) experiments[4,5] observed a phase transition in vanadium characterized as a rhombohedral lattice distortion of the bcc structure at ~ 35 GPa–69 GPa. Shock wave reverse-impact experiment[6] also observed a discontinuity in the sound velocity against the shock pressure at ~ 60.5 GPa. Further first-principles electronic-structure calculations[7–9] elaborated the transition mechanism of the high-pressure rhombohedral phases. For tantalum, an inelastic x-ray scattering (IXS) experiment[10] showed a softening in the aggregate shear velocity in the 90 GPa–100 GPa range, and a typical pressure dependence is restored when above 120 GPa. This behavior is similar to the theoretically predicted pressure dependence of the shear modulus. However, for niobium, so far there is no experimental evidence to support the predicted shear modulus anomaly.

The shear modulus sets a natural scale for yield strength in the framework of the theory of dislocations,[11] so this extraordinary softening of the shear modulus of the VB metals might lead to an unusual effect on the yield strength and other mechanical properties at the relevant pressure, even an anomalous softening in the yield strength. The yield strength, the minimum stress that allows one to plastically strain a material, is of great interest partly because of the underlying physical connection with shear modulus. For that reason, the yield strength of the VB metals attracted numerous experimental investigations.[12–16] Klepeis *et al.*[12] observed a decrease in the yield strength of vanadium starting at ~ 40 GPa–50 GPa both in polycrystalline foils and powders, following the softening trend of the shear modulus. Jing *et al.*[13] observed an obvious reduction in the yield strength of tantalum at ~ 52 GPa–69 GPa with typical pressure dependence above 69 GPa, which is in accordance with the softening trend of the shear modulus by theoretical prediction[3] and IXS measurements.[10] Dewaele *et al.*[14] measured the yield strength of single crystal tantalum up to 93 GPa. In the two experimental runs, they observed a distinct yield strength decrease at above 51 GPa and 84 GPa, respectively. Considering the possible orientation difference between the single crystals used in the two experiment runs, the experimentally observed yield strength decrease still followed the trend of the shear modulus qualitatively.[3,10]

However, in vanadium and tantalum's group VB rel-

*Project supported by the National Natural Science Foundation of China (Grant Nos. U1530134, U1730248, 11772312, and 11504354).

†Corresponding author. E-mail: j_qm@163.com

© 2018 Chinese Physical Society and IOP Publishing Ltd

ative niobium, the measured yield strength in previous experiments[15,16] did not show the expected yield strength softening under pressure. Using the radial XRD method[17] in combination with the lattice strain theory[18,19] and the line-width analysis method,[20–25] the yield strength of niobium was experimentally investigated up to 40 GPa.[15,16] The experiment results showed that the yield strength of niobium initially increases with pressure and follows a subtle decrease with a shallow maximum at $\sim$ 12 GPa–13 GPa, and then restored a monotonic increase beyond 13 GPa (the decrease in "yield strength" below 13 GPa may be in connection with the yielding of the initial sample, as discussed in Section 4). The discrepancy between the experimental observation[15,16] and the theoretical prediction[1–3] motivates us to revisit the yield strength of niobium at high pressures.

In this work, the yield strength of pure niobium powder is determined up to 61 GPa at room temperature using the diamond anvil cell (DAC) combined with synchrotron angle-dispersive x-ray diffraction. An obvious strength softening in niobium is observed. Our experiment provides data to validate theoretical models and to develop insights into the fundamental physical mechanisms controlling the pressure-dependent yield strength of niobium.

2. Theoretical analysis

The stress state of polycrystalline sample, nonhydrostatically compressed between two diamond anvils of DACs, is generally considered as a superposition of a macroscopic differential stress and a microscopic deviatoric stress,[20] which result in macro- and micro-strains, respectively. The microscopic strain causes the broadening of the diffraction lines and the macroscopic one leads to the diffraction lines shifting. The broadening and shift of the diffraction lines is valuable information for the mechanical properties of the sample. The diffraction-line broadening, an indicator of the distribution of the longitudinal micro-strain parallel to the diffraction vector, is used to analyze and to extract the high-pressure yield strength. This method is termed as the line-width analysis method.[16,21–25] In the framework of the line-width analysis theory, the diffraction-line broadening due to microscopic deviatoric strain and crystallite size varies with diffraction angle under angle-dispersive x-ray diffraction geometry as[21,22]

$$2w_{\mathrm{S}}(2\theta) = K\lambda/(L\cos\theta), \tag{1}$$

$$2w_{\mathrm{D}}(2\theta) = 4\eta\tan\theta, \tag{2}$$

where $2w_{\mathrm{S}}(2\theta)$ and $2w_{\mathrm{D}}(2\theta)$ represent the line broadening from the grain size and lattice distortion contributions, respectively, 2θ is the diffraction angle, K is the Scherrer constant, λ is the x-ray wavelength, L is the average grain size, and η is the microscopic deviatoric strain distribution parallel to the diffraction vector. The combined strain and size broadening in the case of Gaussian profiles is given as[21,22]

$$(2w_{hkl}\cos\theta_{hkl})^2 = (K\lambda/L)^2 + \eta_{hkl}^2\sin^2\theta_{hkl}, \tag{3}$$

where $(2w_{hkl})$ denotes line broadening on 2θ-scale, θ_{hkl} is the Bragg angle of reflection (hkl), and η_{hkl} the microscopic deviatoric strain perpendicular to the diffraction plane (hkl). Equation (3) can be rewritten in terms of the single-crystal Young modulus E_{hkl} as[16]

$$(2w_{hkl}\cos\theta_{hkl})^2 = (K\lambda/L)^2 + [4\nu/E(hkl)]^2\sin^2\theta_{hkl}, \tag{4}$$

where ν is the microscopic deviatoric stress. Once a sample suffers plastic deformation and yields, ν can interpreted as the yield strength of the polycrystalline sample. Equation (4) suggests that the $(2w_{hkl}\cos\theta_{hkl})^2$ versus $[\sin\theta_{hkl}/E(hkl)]^2$ plot is a straight line with a slope of $(4\nu)^2$ and the ordinate intercept of $(K\lambda/L)^2$, from which ν and L can be calculated.

For a cubic system,

$$1/E(hkl) = S_{11} - 2(S_{11} - S_{12} - S_{44}/2)\Gamma(hkl), \tag{5}$$

where S_{ij} are the single-crystal elastic compliances, and

$$\Gamma(hkl) = (h^2k^2 + k^2l^2 + l^2h^2)/(h^2 + k^2 + l^2)^2. \tag{6}$$

S_{ij} can be expressed in terms of the single-crystal elastic constants C_{ij} as

$$S_{11} = (C_{11} + C_{12})/(C_{11} - C_{12})/(C_{11} + 2\,C_{12}), \tag{7}$$

$$S_{12} = (-C_{12})/(C_{11} - C_{12})/(C_{11} + 2C_{12}), \tag{8}$$

$$S_{44} = 1/C_{44}. \tag{9}$$

C_{ij} is usually extrapolated with the relationship[26]

$$C_{ij} = C_{ij}^0 + (\mathrm{d}C_{ij}/\mathrm{d}P)\times P\times (V/V_0)^{1/3}, \tag{10}$$

where C_{ij}^0 are the value at ambient conditions, $(\mathrm{d}C_{ij}/\mathrm{d}P)$ are their first-order pressure derivative at ambient conditions, P is pressure, while V and V_0 denote the volume at high pressure and ambient conditions, respectively. For niobium, $(\mathrm{d}C_{ij}/\mathrm{d}P)$ and C_{ij}^0 used in this work are taken from Ref. [27] and listed in Table 1.

Table 1. The single-crystal elastic constants C_{ij}^0 and the first-order pressure derivatives $(\mathrm{d}C_{ij}/\mathrm{d}P)$.[27]

C_{11}^0/GPa	C_{12}^0/GPa	C_{44}^0/GPa	$(\mathrm{d}C_{11}/\mathrm{d}P)$	$(\mathrm{d}C_{12}/\mathrm{d}P)$	$(\mathrm{d}C_{44}/\mathrm{d}P)$
246.2	132.9	28.7	5.22	3.37	0.281

3. Experimental detail

The experiment was performed with 300-μm-diameter flat diamond anvils mounted in a modified Mao–Bell symmetric DAC. A rhenium gasket, pre-indented from an original thickness of 250 μm to $\sim$ 30 μm and drilled an $\sim$ 80-μm-diameter hole, was packed with the commercial polycrystalline niobium powders (99.9% purity, Alfa Aesar, a typical particle size of about 2 μm). A 5-μm ruby chip was

loaded at the center of the niobium sample as a pressure marker.[28] A schematic diagram of the experimental configuration is shown in Fig. 1. To maximize the nonhydrostatic stress, no pressure media was employed in the experiment. Angle-dispersive x-ray diffraction experiments were conducted at the 4W2 High-Pressure Station of the Beijing Synchrotron Radiation Facility (BSRF). An incident x-ray beam, with a wavelength of 0.6199 Å monochromatized by a double crystal (silicon 220), was focused to a size of 15 (vertical) $\times$28 (horizontal) μm^2 of the full width at half maximum (FWHM) by using Kirkpatrick–Baez mirrors. The incident x-ray beam covers the whole ruby chip as shown in Fig. 1 to make sure that the measured pressure by ruby can reliably represent the pressure of the diffracted sample. The diffraction patterns were recorded with an MAR345 on-line image plate with a typical exposure time varying between 5 min–10 min. The distance between the detector and niobium sample, as well as the detector tilt, was calibrated by the CeO_2 standard from the National Institute of Standards and Technology (NIST). All experiments were conducted at ambient temperature. The collected two dimensional images were integrated using the Fit2D program[29] to give the intensity versus 2θ diffraction profiles. The FWHM and 2θ of each diffraction line were then obtained by fitting the diffraction profiles using the PeakFit program. Refinement of bcc and possible rhombohedral structure were conducted using EXPGUI GSAS.[30] By assuming that the ambient width of the diffraction lines include the instrument response and sample response as Zhang *et al.*[31] suggested, the broadening due to microscopic deviatoric strain at high pressures was then derived.

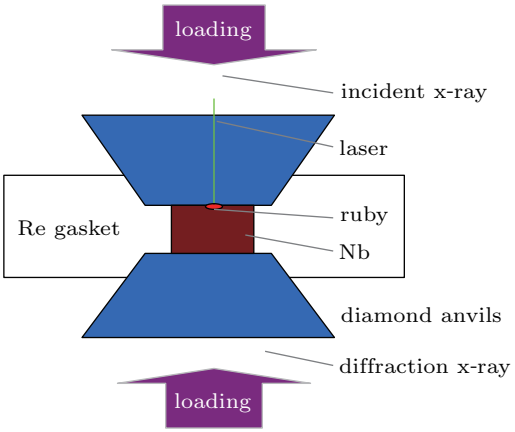


Fig. 1. (color online) The schematic diagram of the experimental configuration. The incident x-ray beam covers the whole ruby chip. The diamond anvils apply a uniaxial loading on the niobium sample, and the rhenium gasket makes a radial restriction on the sample.

4. Results and discussion

Typical results of fitting Eq. (4) to the line-width data are shown in Fig. 2. Though only (110), (200), and (211) reflections from niobium were measured at all scanned high pressures because of the limited angular aperture of the DAC, the linear fittings as shown in Fig. 2 demonstrate a good accuracy. The slope of the fitting lines (solid lines) increases with pressure but for those between 42 GPa–47 GPa, which (indicated by the dashed lines) displays a decreasing trend at elevating pressures.

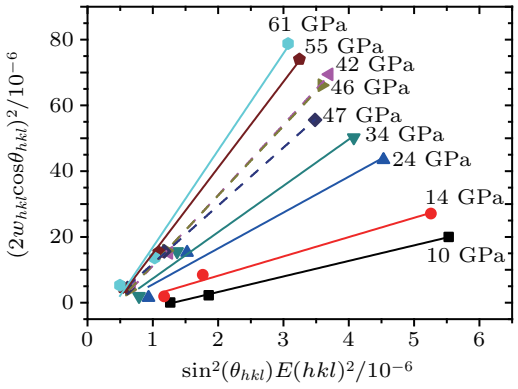


Fig. 2. (color online) Some typical results of fitting Eq. (4) to the measured line width-data. The experimental data are denoted by solid symbols and the straight lines are the fitting lines.

The microscopic deviatoric stress, calculated by the slope $[4\nu/E(hkl)]^2$ and single-crystal Young's modulus E_{hkl}, are shown in Fig. 3 as a function of pressure. For comparison, the experiment data from the microscopic deviatoric stress analysis[16] (S2015-1, fitting using Eq. (4), solid squares), the microscopic deviatoric strain analysis[16] (S2015-2, fitting using Eq. (3), asterisks), and the radial XRD method[15] (S2011, solid triangles) are also included in Fig. 3. It can be seen that our results have a good agreement with the data of S2015-1 and S2015-2, but are somewhat larger than the data of S2011. The data S2015-2 show a much larger scattering.

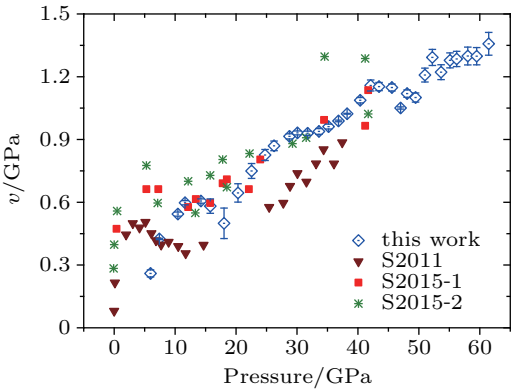


Fig. 3. (color online) The microscopic deviatoric stress as a function of pressure. The experimental data measured in this work are denoted by the open diamonds. Those of Ref. [16] obtained from microscopic deviatoric stress analysis (S2015-1) and microscopic deviatoric strain analysis (S2015-2) are denoted by the solid squares and asterisks, respectively. Those of Ref. [15] (S2011) are denoted by the solid triangles.

The good quality of our data unequivocally indicates that there are three unusual regimes in the microscopic deviatoric stress versus pressure plot as shown in Fig. 3. The first one is from 14 GPa to 18 GPa, where the microscopic deviatoric stress continuously decreases and reaches a shallow minimum. It is not difficult to find in Fig. 3 that a similar decrease in

yield strength also presents in other results[15,16] as between 6 GPa–12 GPa. Generally, by applying a uniaxial load, the stress in conventional bcc metals continuously increases up to its elastic limit and then follows a slight decrease. This change corresponds to the material yield that is characterized by a stress oscillation due to plastic deformation. This phenomenon was also observed in tantalum, molybdenum, and tungsten[32] at high pressure. In our experiment, the microscopic deviatoric stress in the niobium sample increases from zero at ambient condition to the elastic limit upon compression and then yields with the typical characteristics of stress reduction and oscillation at 14 GPa∼ 18 GPa, which could be verified by the large error bar in the microscopic deviatoric stress near 18 GPa, as shown in Fig. 3. So we conclude that the reduction of the microscopic deviatoric stress of niobium in this regime can be attributed to the sample yielding. This interpretation is also applicable to the decreasing process in the "yield strength" of niobium between 6 GPa–12 GPa found in previous studies[15,16] since the same loading method was employed. The different yielding pressures in these results may be attributed to the different initial samples used in these studies. The niobium sample in previous studies[15,16] was cut from a rod in a compact form of the polycrystalline material, whereas the powder sample was used in this work. The powder sample loaded in DAC becomes more efficiently packed firstly and achieves the maxima density above 10 GPa. So it is reasonable to expect that the compact sample would firstly undergo yielding. Beyond yielding, the microscopic deviatoric stress in this work should denote the high-pressure yield strength of niobium.

The second anomalous regime is between 30 GPa–35 GPa and the third one is between 42 GPa–47 GPa. The yield strength indicates a plateau between 30 GPa–35 GPa, and then follows a continuous decrease above 42 GPa, accompanied with a minimum at 47 GPa. The decrease in the yield strength is in accordance with the slopes of the fitting lines, as shown in Fig. 2. Above 47 GPa, a typical pressure dependence is followed. This strength softening is unusual since, as Bridgman[33] observed, strength and ductility in metals commonly was enhanced by applying load/pressure. Several possible mechanisms, applicable to conventional bcc metals, are suggested to account for the pressure-dependent yield strength softening in niobium. Firstly, the pressure induced structural transformation was used to interpret the strength loss in DAC experiments, e.g., the B_1–B_2 transition in NaCl,[34] the stishovite–$CaCl_2$ transition in SiO_2,[35] and especially the bcc-rhombohedral transition in vanadium.[4] To examine the possible structural transformation, we investigated the pressure versus volume data of niobium at 300 K, as displayed in Fig. 4. The solid circles are the experimental data and the solid line is the 3rd order Birch–Murnaughan fitting. The experimental data determined by Takemura *et al.*[36] with helium (Takemura–He, open up-triangles) and methanol–ethanol–water (Takemura–MEW, open right-triangles) pressure media are also included in Fig. 4 for comparison. Our experimental data are somewhat harder than that of Takemura *et al.*[36] but with a much smaller scattering. The 3rd order Birch–Murnaughan fit yields a bulk modulus K_0 of 189(1) GPa and its pressure derivative K_0' of 2.6(0.1), respectively, whereas Takemura *et al.*[36] gives $K_0 = 168(4)$ GPa and $K_0' = 3.4(0.3)$. Considering the nonhydrostatic loading and the possible stress concentration around the ruby chip in this work, the difference in K_0 and K_0' between these two results is reasonable. According to our experiment data, there is no distinct discontinuity in the pressure–volume curve. No evidence of phase transition has been found in previous x-ray diffraction studies too.[3,15,16,37] It should be noted that a phase transition without a perceptible volume change has been observed in vanadium,[4,5] characterized by the broadening and splitting of the (110) and (211) diffraction peaks. To look for a similar phase transition in niobium, we also analyzed all available high-pressure diffraction profiles. A fitting comparison between bcc and rhombohedral structures of niobium at 47 GPa is shown in Fig. 5 as an example. The deviation of the simulated line (solid line) from the experimental data (open circles) at the (211) diffraction line mainly originated from the compressive anisotropy of niobium at high pressure. Refinement of rhombohedral structure ($wRp = 0.0193$, $Rp = 0.0098$) demonstrates a better accuracy than that of bcc structure ($wRp = 0.0307$, $Rp = 0.0151$). However, we could not conclude the existence of a bcc-rhombohedral structure transformation, since it is natural that to fit the diffraction peaks with more lattice planes to take small distortions into account would give a better fitting accuracy, especially in the nonhydrostatic conditions of this work. Furthermore, no resolved splitting peak can be found by observation of the Debye–Scherrer diffraction rings, even though we used a long x-ray wavelength (0.6199 Å) and a large sample-detector distance (∼ 270 mm) to improve the resolution. Additionally, the lattice parameter α of the rhombohedral unit cell does not show a consistent change with pressure as expected in the rhombohedral structure, which varied from 109.729° at 30 GPa to 109.701° at 42 GPa, to 109.711° at 47 GPa, and to 109.641° at 61 GPa. The small departure from the ideal bcc value of 109.47° is not enough to secure it as a rhombohedral phase.[9] Rather, it is more reasonable to interpret it as that the niobium lattice suffers a trigonal shear and follows a subtle distortion. It is worth noting that recently a very comprehensive theoretical calculation[38] showed that niobium does not show any structure change in that pressure range. Their proposed two softest distortions, along RH1 at 39 GPa and RH2 at 61 GPa, respectively,[38] are in good accordance with our ob-

served softening in the yield strength at 30 GPa and 47 GPa, as shown in Fig. 3. As for the anisotropic broadening of the diffraction peaks (110) and (211) at high pressures, it may be related to the strong uniaxial stress of niobium under nonhydrostatic compression. Takemura *et al.*[36] performed a detailed analysis of the uniaxial stress component on niobium up to 134 GPa and observed a distinct asymmetry and broadening of (110) and (211) peaks caused by the increasing uniaxial stress. Consequently, niobium does not experience phase transition at least below 61 GPa, and its yield strength softening is not an indicator of phase change.

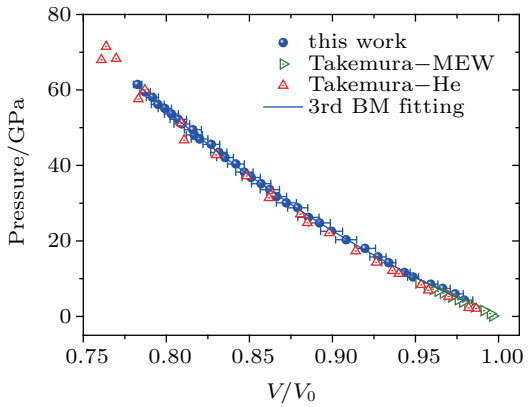


Fig. 4. (color online) Pressure versus volume data for niobium at 300 K. The solid circles are the experimental data measured under nonhydrostatic conditions in this work and the solid line is the 3rd order Birch–Murnaughan fit. The open up-triangles and right-triangles are the experimental data determined by Takemura *et al.*[36] in helium (Takemura–He,) and methanol–ethanol–water (Takemura–MEW) pressure media, respectively. No distinct discontinuity in pressure–volume was observed.

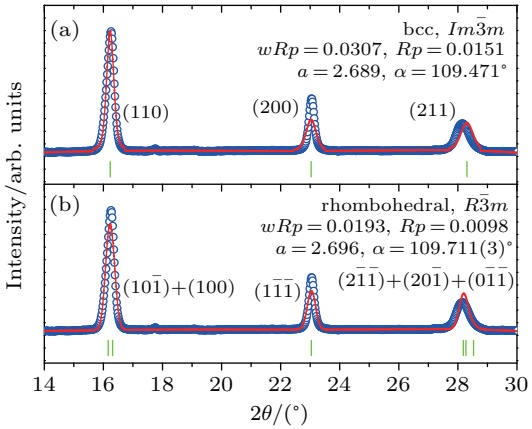


Fig. 5. (color online) A fitting comparison between bcc (a) and rhombohedral (b) structures of niobium at 47 GPa. The circles are the integrated diffraction patterns of niobium and the solid lines are the calculated patterns. The short vertical lines label the 2θ location of diffraction peaks. The crystal structure, space group, fitting results, and lattice parameter α of the unit cell are shown in the right-upper panel. No resolved splitting peaks were observed at all pressures.

Some researchers[39,40] advised that the texture/preferred orientation of the sample at high pressures could lead to the strain softening. The preferred orientation/texture could be indicated by a non-uniform distribution or changes in the intensity of the Debye–Scherrer diffraction rings.[12] Figure 6 shows the segments of the diffraction patterns of the niobium at 18, 35, 46, and 61 GPa recorded by the Mar345 image plate. The signal intensities do not change significantly relative to the rest of the arcs as the pressure increases, which may suggest that the degree of preferred crystallographic orientation in niobium is not so notable at high pressures. However, it should be noted that it is important to record the full diffraction rings in any diffraction geometry before concluding the presence or absence of texture.

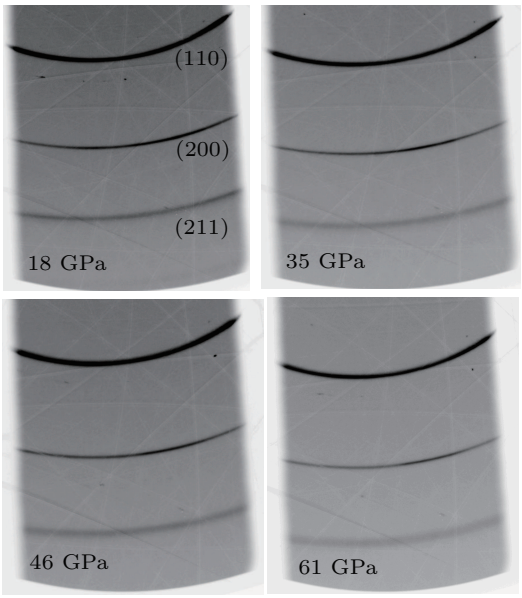


Fig. 6. X-ray diffraction patterns of a niobium powder sample at 18, 35, 46, and 61 GPa on MAR345 image plate.

Meade and Jeanloz[39] found the yield strength of MgO varies with the different initial thickness of the sample (thus different strain at high pressures) and attributed it to the preferred orientation of MgO. However, in one of their independent experiment runs, the yield strength of MgO monotonously increased with elevating pressures, which is essentially different from how niobium behaves in this work. Furthermore, the effect of the preferred orientation is a continuously smooth function of pressure,[41] and the yield strength-pressure curve would level out once the texture saturated,[42,43] which cannot interpret the observed decrease in yield strength of niobium. Additionally, the texture/preferred orientation in materials with bcc structure is not so remarkable as those with face centered cubic structure because of the reduction of slip systems, but the observed softening of the yield strength in niobium was more than 15%, an amount even significantly larger than the reported critical case of hcp-Co,[42,43] which is a highly anisotropic material. Weir *et al.*[40] not only observed similar strain softening in Ta samples with different initial thickness as that in MgO,[39] but a notable falling of yield strength in each independent experimental run. They attributed this yield strength anomaly to material damage induced in highly strained specimens. A finite

element modeling[44] revealed that the continuous decrease of high-pressure yield strength of tantalum[40] could be caused by unexpected influence from the cupping of the diamond anvils. Nevertheless, Jing *et al.*[13] found that the yield strength of tantalum decreases at $\sim$ 52 GPa–69 GPa but followed a continuous increase from 69 GPa till the highest pressure 101 GPa, which can never be interpreted by material damage or cupping of diamond anvils. Obviously, the decrease of yield strength in niobium is quite different from the cases in MgO[39] and Ta.[40] Both strain softening and cupping of diamond anvils fail to explain the yield strength variation with pressure, especially the decrease in yield strength above 42 GPa along with a continuous increase.

In the Steinberg strength model,[45] the strain and pressure are the major factors to affect the high-pressure yield strength at room temperature. They both enhance the yield strength at relatively low pressures, whereas the strain hardening component is dominant and constrained by setting the yield strength to an upper limit. After saturation of the plastic strain, the pressure hardening component is the dominant hardening mechanism. The corresponding typical characteristics is that the yield strength versus pressure curve has an initially larger slope followed by a smaller one, such as in lithium fluoride.[46] In this work, the anomalous softening of yield strength in niobium is above 42 GPa, a pressure far beyond the plastic strain it saturates at, and pressure hardening is dominant. Therefore, it is not unreasonable to conclude that the anomalous softening of yield strength in niobium is pressure dependent and caused by the pressure softening of the shear modulus. A theoretical investigation suggested that the latter could be a combined effect of Fermi surface nesting, band John–Teller effects, and electronic topological transition in this pressure range.[38] Our further confidence to make such a conclusion is from the support of niobium's group VB relatives, vanadium and tantalum. An unusual yield strength decrease under pressure was also observed in vanadium[12] and tantalum[13,14] and followed the trend of the predicted shear modulus softening by theoretical studies.[1–3] It should be noted that the theoretical calculation of shear modulus is on the basis of single crystal, whereas the experimental measurement is from the powder sample. A comparison between these results is in principle valid, but the differences should exist to a certain extent. That is why the experimentally observed yield strength softening of VB metals[12–14] qualitatively agree with the predicted shear modulus softening.[1–3,9] The analogous characteristics of yield strength softening in vanadium and tantalum and their consistence with the theoretical prediction make us more confident to believe that the pressure- dependent softening of yield strength in niobium has a close connection with the unusual behavior of the trigonal shear modulus.

5. Conclusions

In conclusion, the microscopic deviatoric stress of niobium has been experimentally investigated up to 61 GPa. Three distinct anomalous regimes were observed. Between 14 GPa–18 GPa, the microscopic deviatoric stress slightly decreased with pressure due to yielding of the packed niobium powder sample. Above 18 GPa, the microscopic deviatoric stress can denote the yield strength of the polycrystalline niobium. The second anomalous regime is from 32 GPa to 35 GPa, where the yield strength levels out. The strongest softening is observed from 42 GPa to 47 GPa, where the yield strength evidently decreases with pressure. The comprehensive analysis shows that the yield strength softening in niobium is independent of phase transition, strain softening caused by preferred orientation (along with material damage), and the cupping of diamond anvils. The experimentally determined pressure-dependent yield strength of niobium behaves similarly to the theoretically predicted pressure-dependent trigonal shear modulus. We argue that there is a systematic relationship between the anomalous strength softening of niobium and the unusual softening in the shear modulus. Further experimental evidence from quantitative texture/preferred orientation analysis and IXS measurement will be helpful to evaluate the strain effect and to determine the pressure dependence of the shear modulus in the concerned pressure range, respectively.

Acknowledgment

The authors appreciate their helpful discussions with Prof. Ji-an Xu and thank Drs. Xiaodong Li, Dongliang Yang, and Yu Gong for their experimental assistance. Experiments were conducted at the 4W2 High-Pressure Station of Beijing's Synchrotron Radiation Facility, which is supported by the Chinese Academy of Sciences (Grant Nos. KJCX2-SW-N03 and KJCX2-SW-N20).

References

[1] Landa A, Klepeis J, Söderlind P, Naumov I, Velikokhatnyi O, Vitos L and Ruban A 2006 *J. Phys.: Condens. Matter* **18** 5079
[2] Landa A, Klepeis J, Söderlind P, Naumov I, Velikokhatnyi O, Vitos L and Ruban A 2006 *J. Phys. Chem. Solids* **67** 2056
[3] Landa A, Söderlind P, Ruban A, Peil O E and Vitos L 2009 *Phys. Rev. Lett.* **103** 235501
[4] Ding Y, Ahuja R, Shu J, Chow P, Luo W and Mao H K 2007 *Phys. Rev. Lett.* **98** 085502
[5] Jenei Z, Liermann H P, Cynn H, Klepeis J H P, Baer B J and Evans W J 2011 *Phys. Rev. B* **83** 054101
[6] Yu Y, Tan Y, Dai C, Li X, Li Y, Wu Q and Tan H 2014 *Appl. Phys. Lett.* **105** 201910
[7] Lee B, Rudd R E, Klepeis J E, Söderlind P and Landa A 2007 *Phys. Rev. B* **75** 180101
[8] Krasilnikov O M, Vekilov Y K, Mosyagin I Y, Isaev E I and Bondarenko N G 2012 *J. Phys.: Condens. Matter* **24** 195402
[9] Wang Y X, Wu Q, Chen X R and Geng H 2016 *Sci. Rep.* **6** 32419
[10] Antonangeli D, Farber D L, Said A H, Benedetti L R, Aracne C M, Landa A, Söderlind P and Klepeis J E 2010 *Phys. Rev. B* **82** 132101

[11] Yang L H, Söderlind P and Moriarty J A 2001 *Mater. Sci. Eng. A* **309–310** 102
[12] Klepeis J H P, Cynn H, Evans W J, Rudd R E and Yang L H 2010 *Phys. Rev. B* **81** 134107
[13] Jing Q, Wu Q, Xu J, Bi Y, Liu L, Liu S, Zhang Y and Geng H 2015 *J. Appl. Phys.* **117** 055903
[14] Dewaele A and Loubeyre P 2005 *Phys. Rev. B* **72** 134106
[15] Singh A K and Liermann H P 2011 *J. Appl. Phys.* **109** 113539
[16] Singh A K and Liermann H P 2015 *J. Appl. Phys.* **118** 065903
[17] Mao H K, Shu J, Shen G, Hemley R J, Li B and Singh A K 1998 *Nature* **396** 741
[18] Singh A K 1993 *J. Appl. Phys.* **73** 4278
[19] Singh A K 2009 *J. Appl. Phys.* **106** 043514
[20] Weidner D J, Wang Y and Vaughan M T 1994 *Geophys. Res. Lett.* **21** 753
[21] Langford J I 1971 *J. Appl. Crystallogr.* **4** 164
[22] Gerward L, Morup S and Topsoe H 1976 *J. Appl. Phys.* **47** 822
[23] Singh A K, Liermann H P and Saxena S K 2004 *Solid State Commun.* **132** 795
[24] Singh A K, Liermann H P, Akahama Y and Kawamura H 2007 *J. Appl. Phys.* **101** 123526
[25] Liu L, Song H X, Wang Z, Geng H, Jing Q, Zhang Y, Liu S, Xiang S, Bi Y, Xu J, Li Y, Li X and Liu J 2012 *J. Appl. Phys.* **112** 013532
[26] Guinan M and Steinberg D 1975 *J. Phys. Chem. Solids* **36** 829
[27] Katahara K W, Manghnani M H and Fisher E S 1976 *J. Appl. Phys.* **47** 434
[28] Liu L, Bi Y and Xu J 2013 *Chin. Phys. B* **22** 056201
[29] Hammersley A P, Svensson S O, Hanfl, M, Fitch A N and Hausermann D 1996 *High Press. Res.* **14** 235
[30] Toby B H 2001 *J. Appl. Crystallogr.* **34** 210
[31] Zhang J, Wang L, Weidner D J, Uchida T and Xu J 2002 *Am. Mineralogist* **87** 1005
[32] Bridgman P W 1953 *J. Appl. Phys.* **24** 560
[33] Bridgman P W 1935 *Phys. Rev.* **48** 825
[34] Meade C and Jeanloz R 1988 *J. Geophys. Res.* **93** 3270
[35] Shieh S R and Duffy T S 2002 *Phys. Rev. Lett.* **89** 255507
[36] Takemura K and Singh A K 2006 *Phys. Rev. B* **73** 224119
[37] Singh A K and Takemura K 2001 *J. Appl. Phys.* **90** 3269
[38] Wang Y X, Geng H, Wu Q, Chen X R and Sun Y 2017 *J. Appl. Phys.* **122** 235903
[39] Meade C and Jeanloz R 1988 *J. Geophys. Res.* **93** 3261
[40] Weir S T, Akella J, Ruddle C, Goodwin T and Husing L 1998 *Phys. Rev. B* **58** 11258
[41] Bosak A, Krisch M, Fischer I, Huotari S and Monaco G 2007 *Phys. Rev. B* **75** 064106
[42] Merkel S, Miyajima N, Antonangeli D, Fiquet G and Yagi T 2006 *J. Appl. Phys.* **100** 023510
[43] Merkel S, Tomé C and Wenk H R 2009 *Phys. Rev. B* **79** 064110
[44] Jing Q "Finite element modeling on deformation of diamond and gasket under diamond anvil cell loading" (unpublished)
[45] Steinberg D J, Cochran S G and Guinan M W 1980 *J. Appl. Phys.* **51** 1498
[46] Ao T, Knudson M D, Asay J R and Davis J P 2009 *J. Appl. Phys.* **106** 103507